SUPPLEMENTARY INFORMATION

	Dph2 SeMet (iron-free)[#]	Dph2 (iron-free)	Dph2-[4Fe-4S]
Data collection			
Space group	$P2_12_12_1$	$P2_12_12_1$	$P2_12_12_1$
Cell dimensions			
a, *b*, *c* (Å)	58.26, 82.08, 160.42	58.74, 81.87, 160.01	55.70, 80.53, 162.14
α, β, γ (°)	90, 90, 90	90, 90, 90	90, 90, 90
Resolution (Å)	50 – 2.5 (2.59 – 2.50)*	50 – 2.3 (2.38 – 2.30)	50 – 2.1 (2.18 – 2.10)
R_{sym} or R_{merge}	0.050 (0.409)	0.060 (0.296)	0.062 (0.241)
$I / \sigma I$	29.7 (3.2)	24.0 (2.5)	18.5 (2.4)
Completeness (%)	99.7 (98.5)	98.5 (93.7)	94.3 (66.4)
Redundancy	3.8 (3.7)	6.4 (4.7)	3.7 (2.7)
Refinement			
Resolution (Å)		2.3	2.1
No. reflections		36367	41054
R_{work} / R_{free}		0.216/0.254	0.225/0.268
No. atoms			
Protein		5287	5298
Ligand/ion			26
Water		214	280
B-factors			
Protein		48.6	44.9
Ligand/ion			77.7
Water		48.2	47.2
R.m.s deviations			
Bond lengths (Å)		0.007	0.006
Bond angles (°)		1.012	1.292

[#]The Dph2 SeMet data were used for the initial structure determination by SAD phasing but not for the structure refinement.

*Values in parentheses are for the highest-resolution shell. One crystal was used in each case.

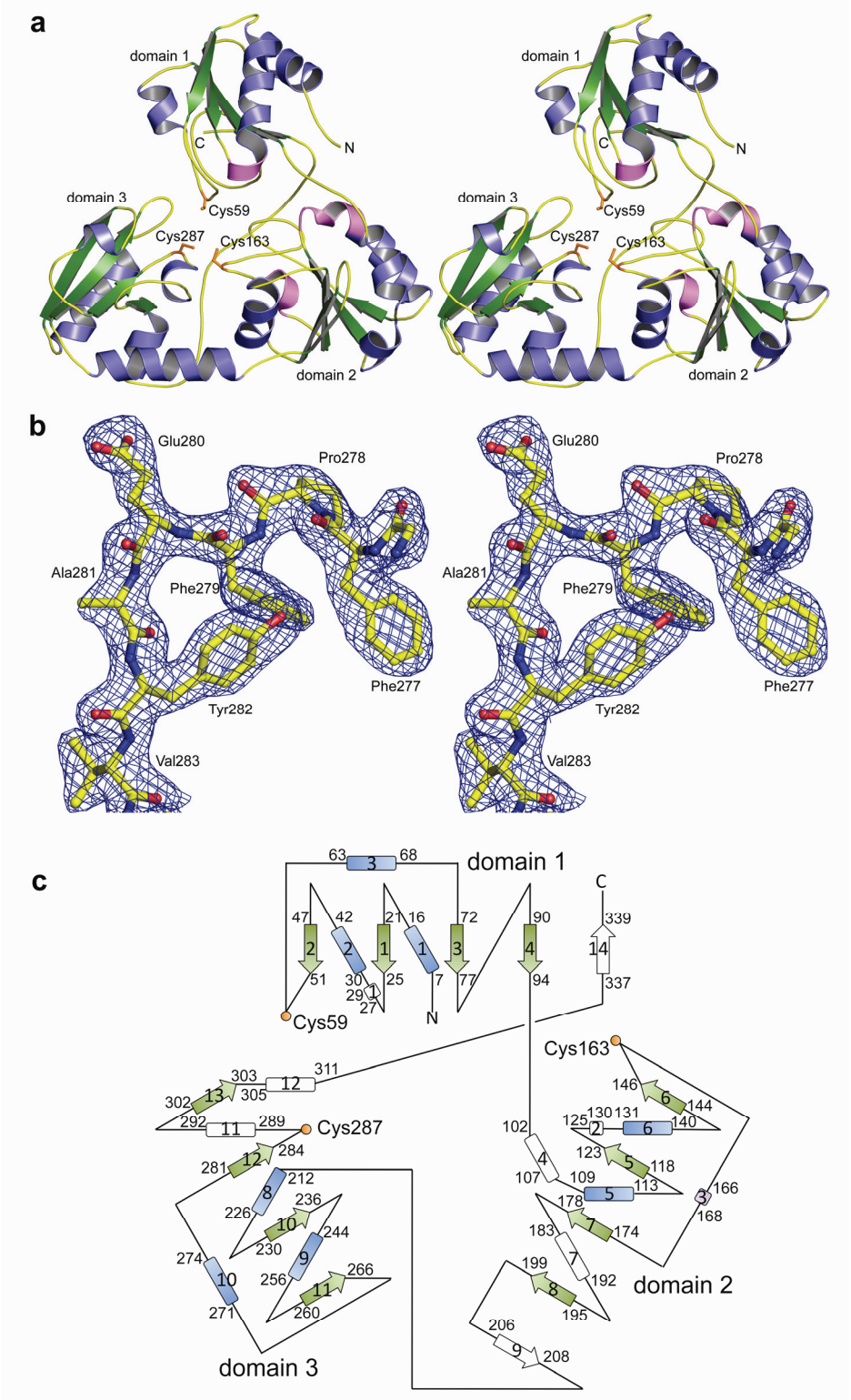

Supplementary Figure 1. Three-dimensional structure of *Ph*Dph2. **a**, *Ph*Dph2 monomer colored by secondary structure. The locations of the three conserved cysteine residues are indicated. **b**, Representative region of a $2F_o$-F_c composite omit electron density map and the final atomic model for residues 277-283. The map was calculated at 2.1 Å resolution and is contoured at 1 σ. **c,** Topology diagram of *Ph*Dph2. The conserved secondary structures of the three domains are colored blue for α-helices, lavender for a 3_{10}-helix, and green for β-strands.

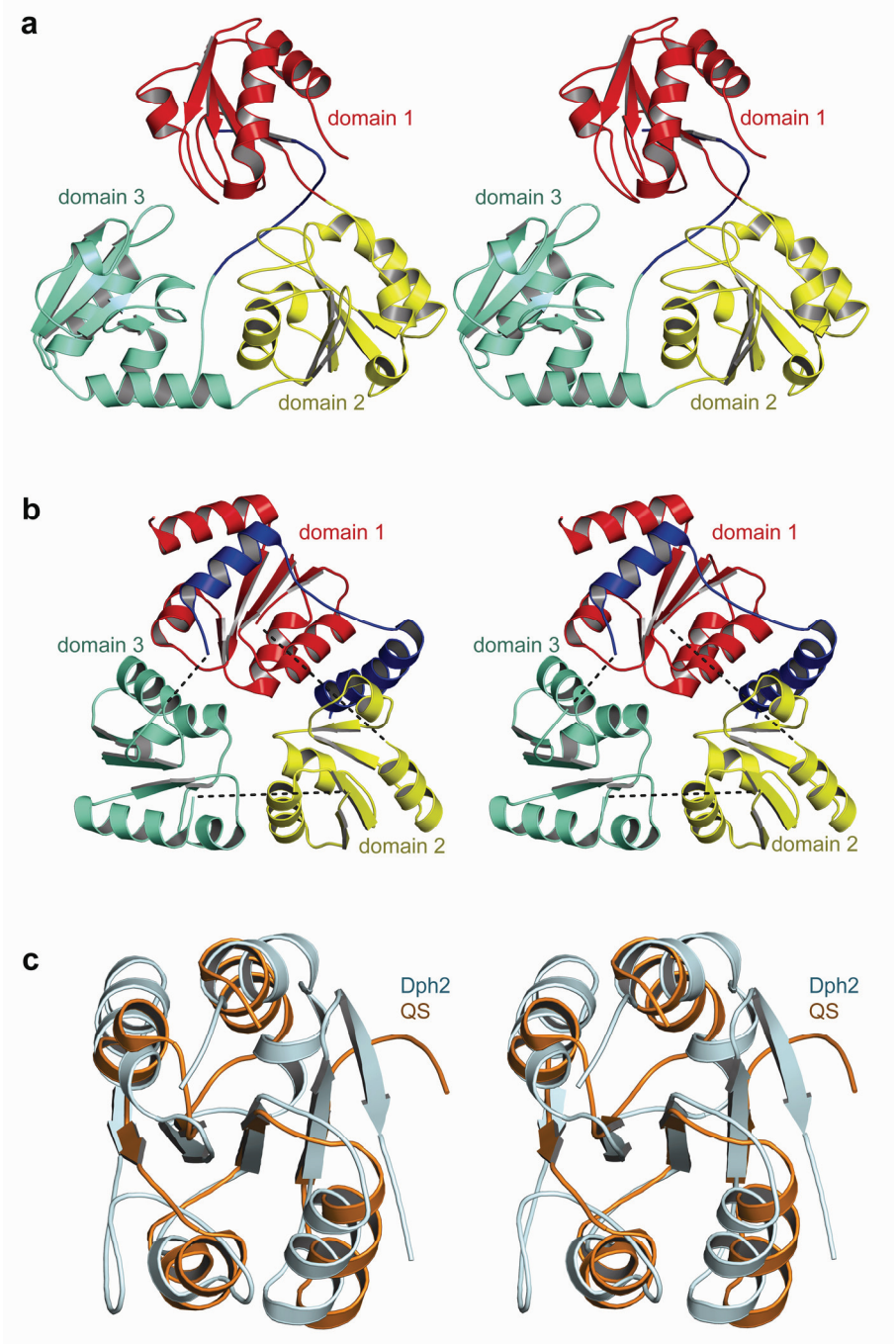

Supplementary Figure 2. Structural comparison of *Ph*Dph2 and *P. horikoshii* quinolinate synthase (QS; PDB ID 1WZU). **a**, Stereoview of a *Ph*Dph2 protomer. **b**, Stereoview of monomeric QS aligned to the orientation of *Ph*Dph2. For each, domain 1 is colored red, domain 2 is colored yellow, domain 3 is colored cyan and the C-terminus is colored blue. All three interdomain connecting loops of QS were disordered in the crystal structure and are indicated in the figure by dashed lines. While the triangular arrangement of three domains is common to both structures, the individual domains of QS are tilted by about 60° with respect to the equivalent domains of *Ph*Dph2. **c**, Stereoview of the superposition of domain 2 from *Ph*Dph2 and domain 2 from QS. *Ph*Dph2 is shown in cyan and QS is shown in orange. The superposition indicates that the domain fold is conserved.

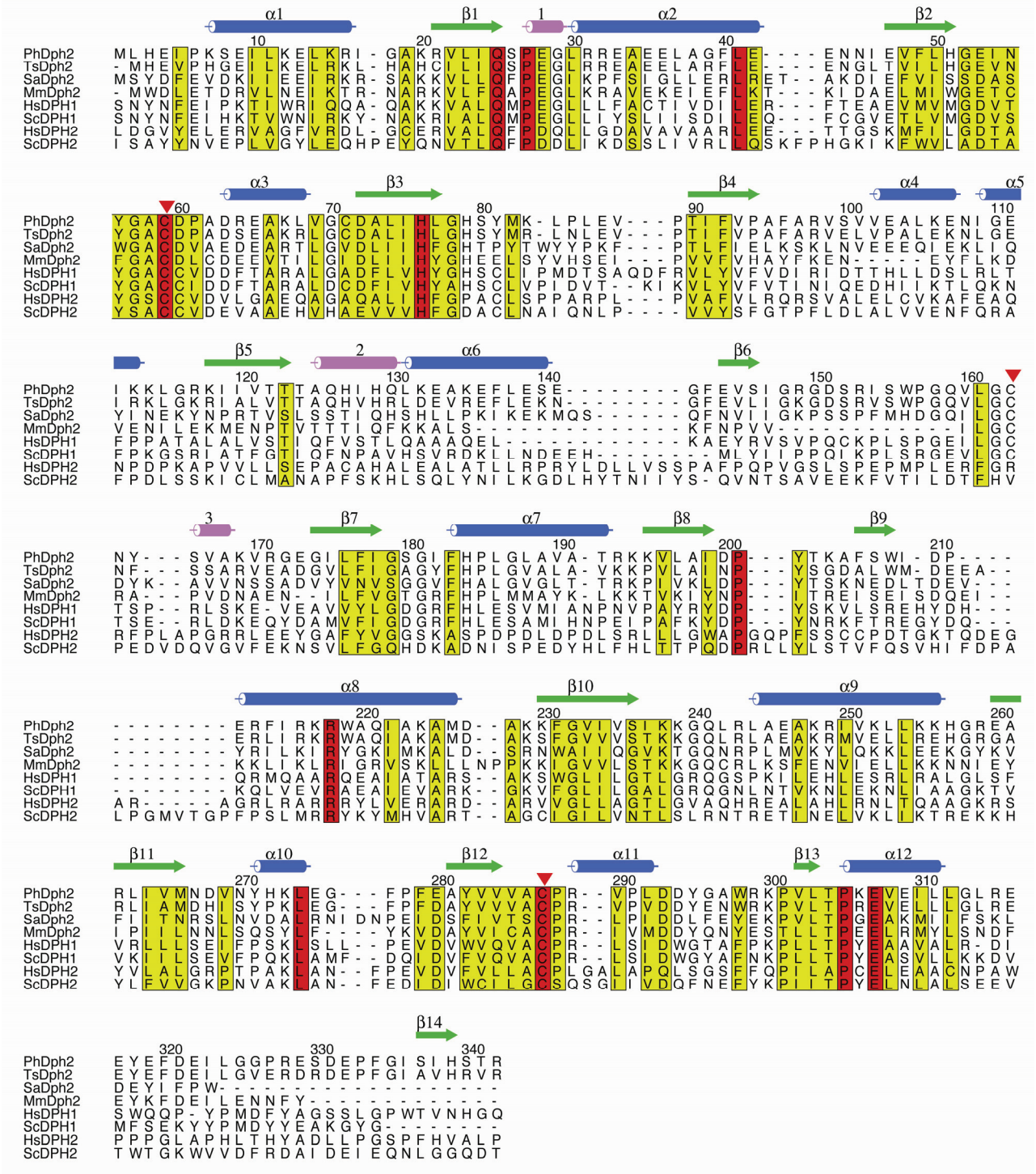

Supplementary Figure 3. Sequence alignment for *Ph*Dph2 and orthologs. Three additional archaeal orthologs are included for comparison: *Thermococcus* sp. AN4 (Ts), *Sulfolobus acidocaldarius* (Sa) and *Methanococcus maripaludis* (Mm). Also included are the *Homo sapiens* (Hs) and *Saccharomyces cerevisiae* (Sc) orthologs of *Ph*Dph2: *Hs*DPH1, *Sc*DPH1, *Hs*DPH2 and *Sc*DPH2. Secondary structural elements are shown above each row and are based on the structure of *Ph*Dph2. Residues conserved in all eight sequences are highlighted in red. Residues with conservative changes are highlighted in yellow. The three conserved cysteine residues that bind to the [4Fe-4S] cluster of *Ph*Dph2 are indicated by red triangles.

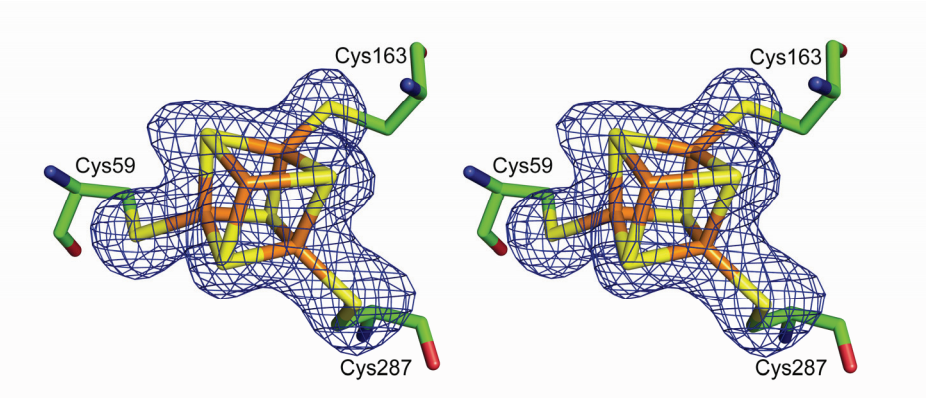

Supplementary Figure 4. Stereoview of electron density corresponding to the [4Fe-4S] cluster. The F_o-F_c electron density map was calculated at 2.1 Å resolution and contoured at 4 σ. Phases for the map were calculated from a model lacking the [4Fe-4S] cluster and the S_β atoms of Cys59, Cys163 and Cys287. The final model for the [4Fe-4S] cluster and the conserved cysteine residues is also shown.

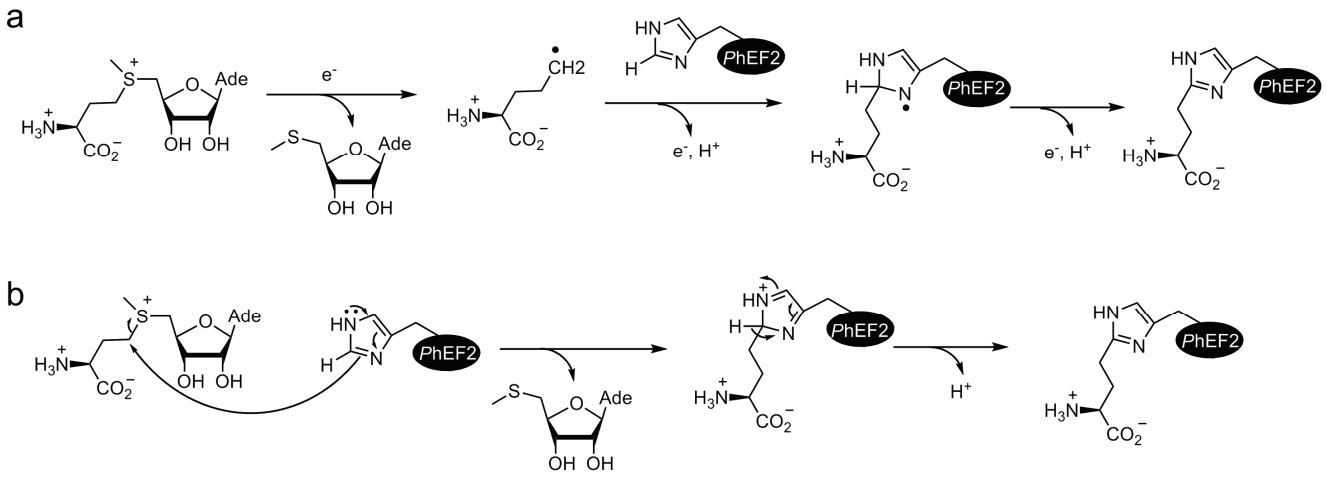

Supplementary Figure 5. Two possible reactions mechanisms proposed for *Ph*Dph2 based on the observation made in Figure 5a. (**a**) A radical mechanism. The $[4Fe\text{-}4S]^+$ cluster provides an electron to reductively break the $C_{\gamma,Met}$-S bond of SAM, generating a 3-amino-3-carboxypropyl radical, which then adds to the imidazole ring. The resulting radical then loses one electron and one proton to give the product. (**b**) A nucleophilic mechanism. The $[4Fe\text{-}4S]^+$ serves to anchor SAM in the right position and orientation for nucleophilic attack by the C2 position of the imidazole ring. Deprotonation of the resulting adduct then gives the product.

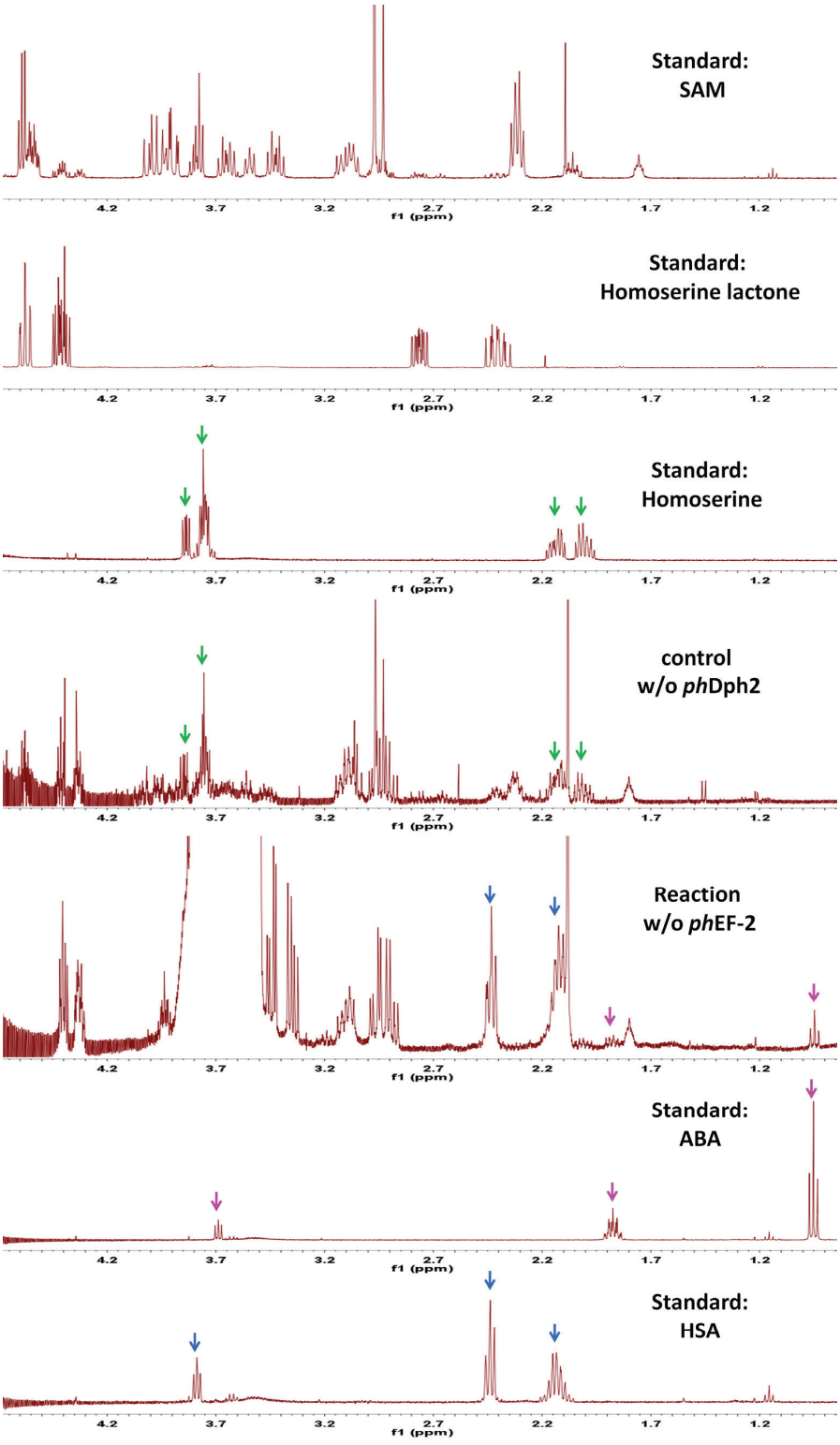

Supplementary Figure 6. NMR spectra of standard compounds, products from *Ph*Dph2 reaction, and products from the control reaction without *Ph*Dph2. These spectra are overlaid so that it is easy to tell which compound is present in the reaction or control. Homoserine lactone (peaks marked with green arrows) and unreacted SAM were the major identifiable compounds present in the control reaction without *Ph*Dph2. In the reaction with *Ph*Dph2, the major identifiable compounds are HSA (peaks marked by cyan arrows) and ABA (peaks marked by magenta arrows).

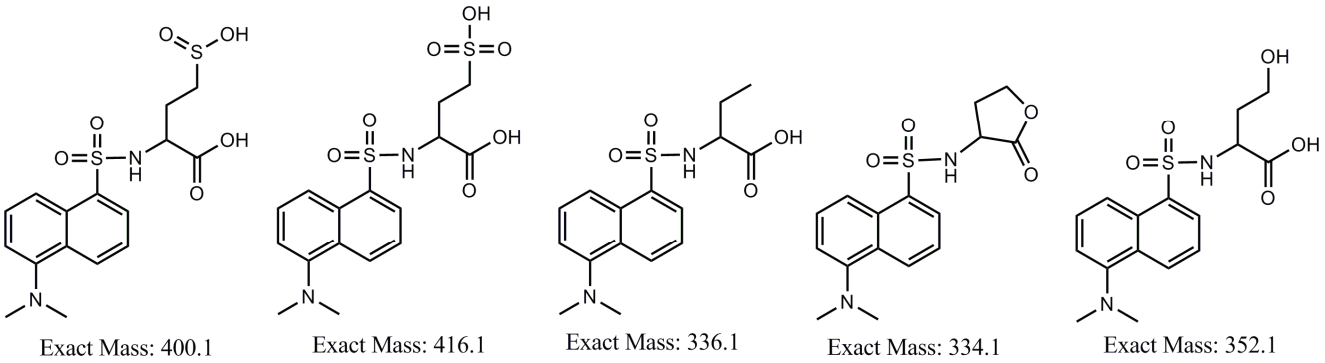

Supplementary Figure 7. The structures and molecular weights of the dansylated compounds that can possibly form in the *Ph*Dph2-catalyzed cleavage of SAM. Whether these compounds were produced or not was checked by LCMS in Figure 5c.

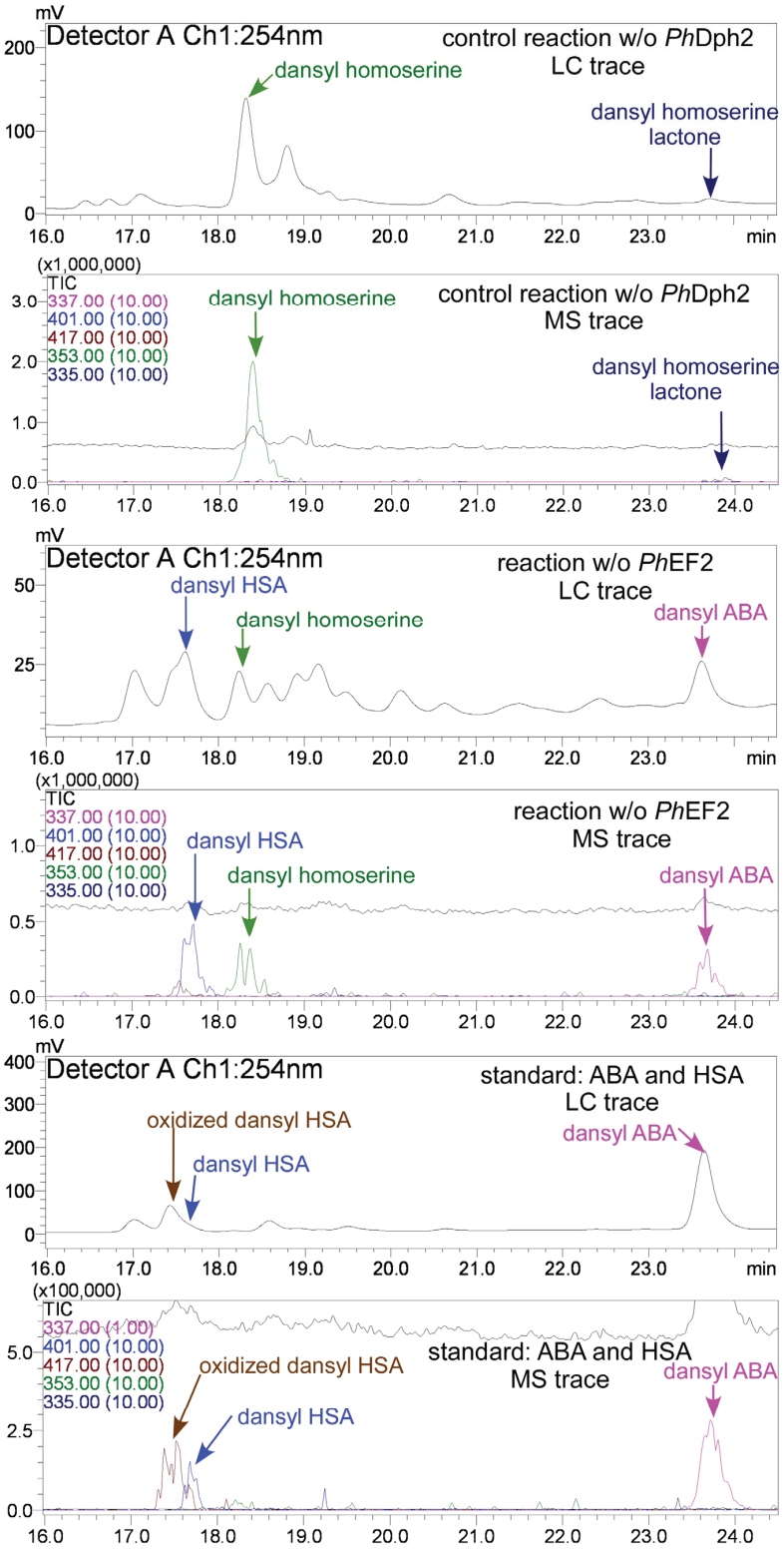

Supplementary Figure 8. Detection of dansylated reaction products in the absence of *Ph*EF2 by LCMS. The LC traces (detected at 254 nm and 335 nm) and MS traces (total ion counts and ion counts for specific compounds) are shown for the reaction with *Ph*Dph2, control reaction without *Ph*Dph2, and ABA and HSA standards. The LC and MS peaks corresponding to dansylated ABA and HSA are marked by arrows.

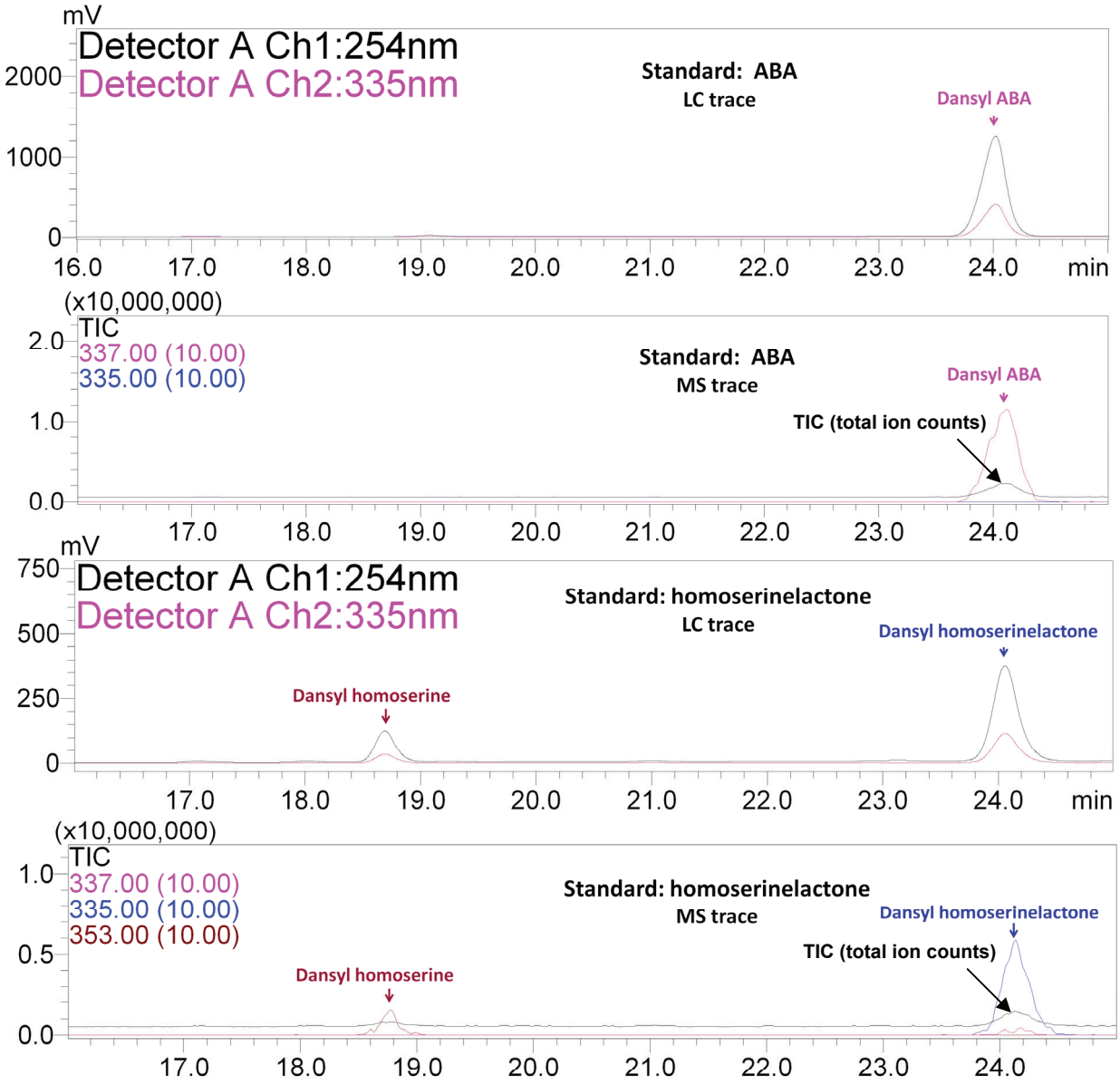

Supplementary Figure 9. The LCMS traces of dansylated ABA (m/z 337), and homoserine lactone (m/z 335) standards. Partial hydrolysis of the homoserine lactone occurred during the dansylation reaction, leading to the formation of dansylated homoserine (m/z 353). Dansylated ABA and homoserine lactone have the same retention time, but their masses are distinct. Dansylated ABA has m/z 337 ions, but no m/z 335 ions. In contrast, dansylated homoserine lactone has strong m/z 335 ions and weak m/z 337 ions due to natural isotope distribution. Thus, the detection of strong m/z 337 ions but weak m/z 335 ions at the desired retention time would suggest the presence of ABA.